Supplementary Information for:

On the nature of active sites for formic acid decomposition on Au catalysts

Sha Li, Suyash Singh, James A. Dumesic, and Manos Mavrikakis*

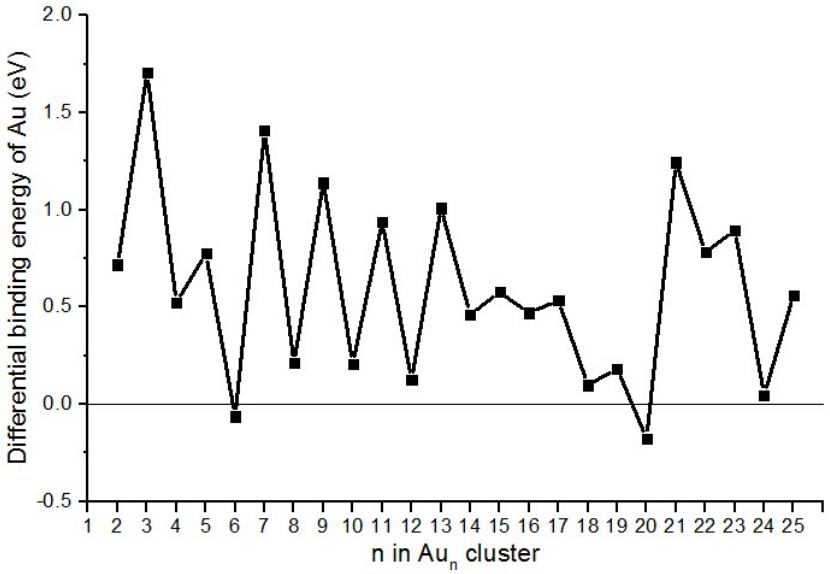

Figure S1 Differential binding energy (dBE) of Au in Au_n (n=2-25) clusters using Au atom in the bulk as the energy reference. dBE = $E(Au_n) - E(Au_{n-1}) - E(Au_{bulk})$.

Table S1 Binding energies of H, COOH, HCOO and HCOOH on Au_n (n=4-25) clusters. BE values on Au(211) are provided for comparison.

	BE(H)	BE(COOH)	BE(HCOO)	BE(HCOOH)
Au_4	-2.39	-2.11	-2.72	-1.02
Au_5	-3.23	-2.58	-3.61	-0.58
Au_6	-1.77	-1.55	-1.92	-0.54
Au_7	-3.31	-2.52	-3.00	-0.65
Au_8	-1.93	-1.68	-2.10	-0.58
Au_9	-2.90	-2.59	-3.16	-0.60
Au_{10}	-2.23	-1.73	-2.47	-0.47
Au_{11}	-2.76	-2.45	-3.00	-0.57
Au_{12}	-2.23	-1.73	-2.49	-0.43
Au_{13}	-2.80	-2.26	-3.01	-0.47

Au_{14}	-2.38	-1.85	-2.49	-0.62
Au_{15}	-2.77	-2.22	-2.87	-0.46
Au_{16}	-2.62	-1.93	-2.71	-0.57
Au_{17}	-2.76	-2.18	-2.82	-0.50
Au_{18}	-2.45	-1.87	-2.81	-0.54
Au_{19}	-2.71	-2.19	-3.03	-0.42
Au_{20}	-1.74	-1.47	-1.95	-0.42
Au_{21}	-2.85	-2.42	-2.94	-0.44
Au_{22}	-2.41	-2.04	-2.71	-0.42
Au_{23}	-2.94	-2.68	-3.25	-0.71
Au_{24}	-2.19	-1.68	-2.74	-0.49
Au_{25}	-2.74	-2.04	-2.78	-0.46
Au(211)	-2.26	-1.63	-2.31	-0.27

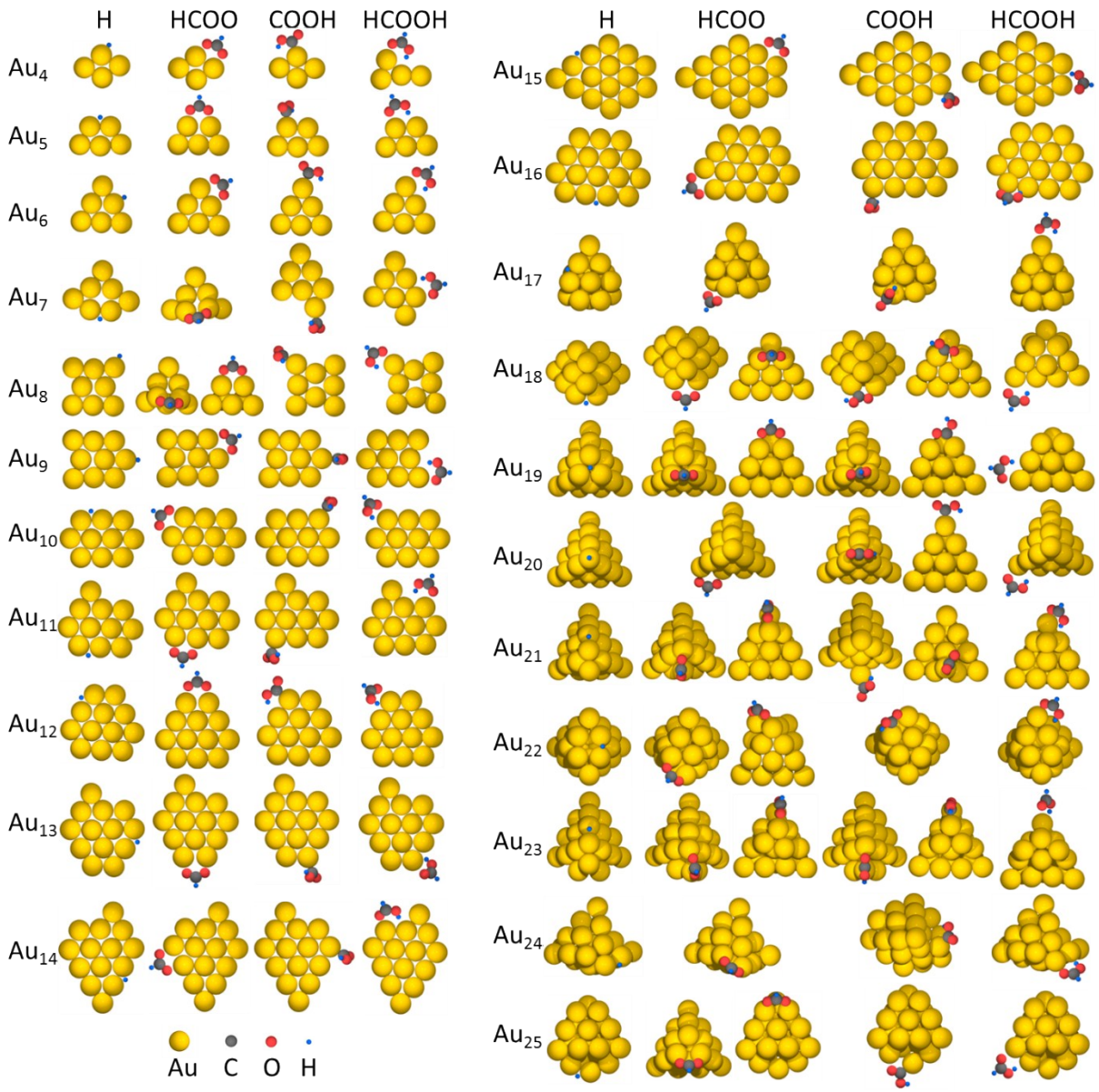

Figure S2 Most stable configurations for H, HCOO, COOH and HCOOH on Au_n (n=4-25) clusters.

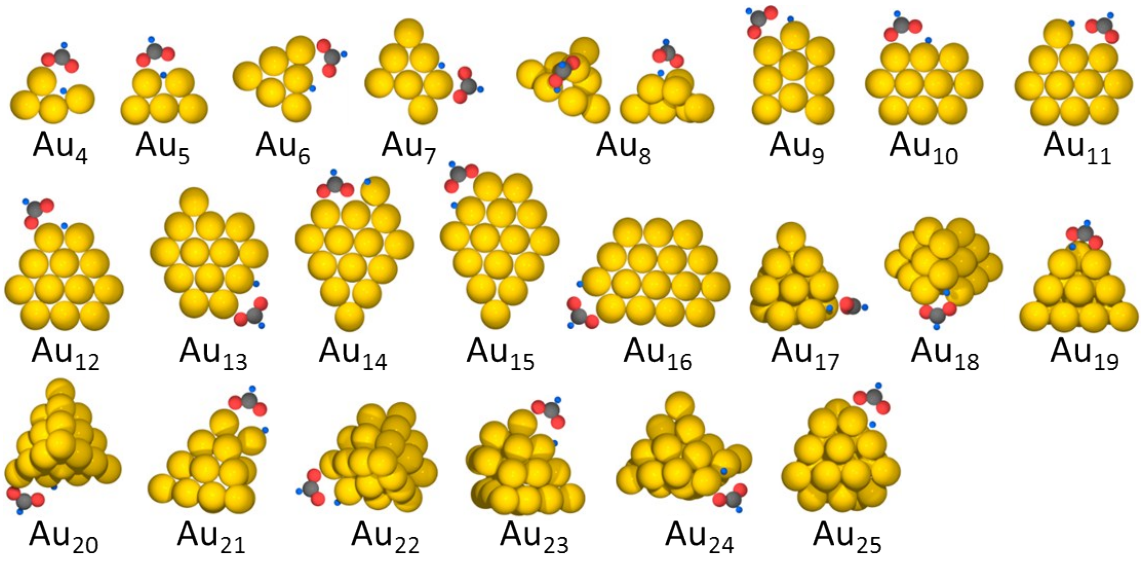

Figure S3 Transition state configurations determined in the minimum energy path for HCOOH dehydrogenation to HCOO on Au_n (n=4-25) clusters.

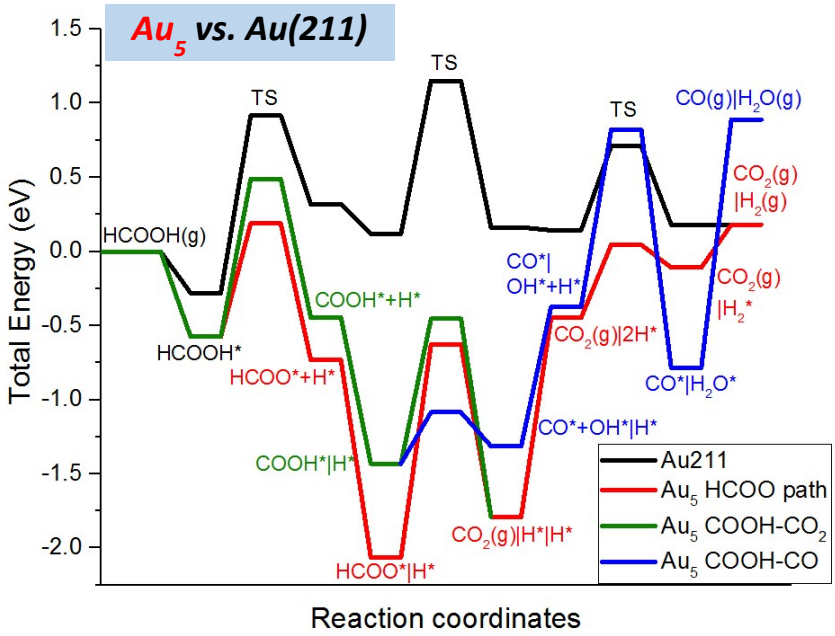

Figure S4 Potential energy diagram (PED) of HCOOH decomposition through the HCOO path (red line), COOH path leading to CO_2 formation (COOH-CO_2 path; green line) and COOH path leading to CO formation (COOH-CO path; blue line) on Au_5. PED for the HCOO path on Au(211) is shown in black, for comparison.

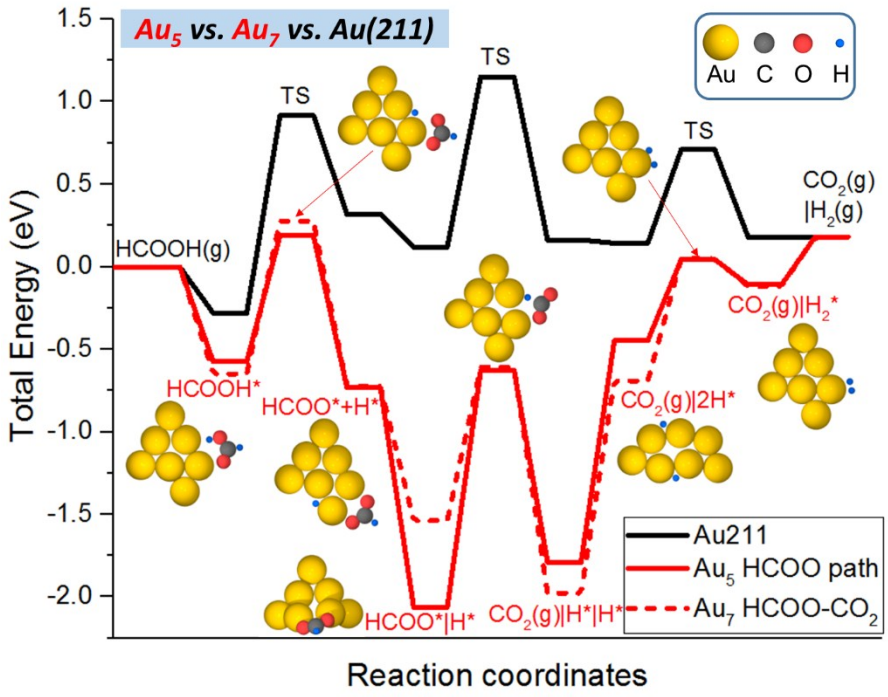

Figure S5 Potential energy diagram (PED) of HCOOH decomposition through the HCOO path on Au_5 (solid red line) and Au_7 (dashed red line). PED for Au(211) is shown in black, for comparison. Insets show configurations of the most favorable adsorbed states and transition states on Au_7.

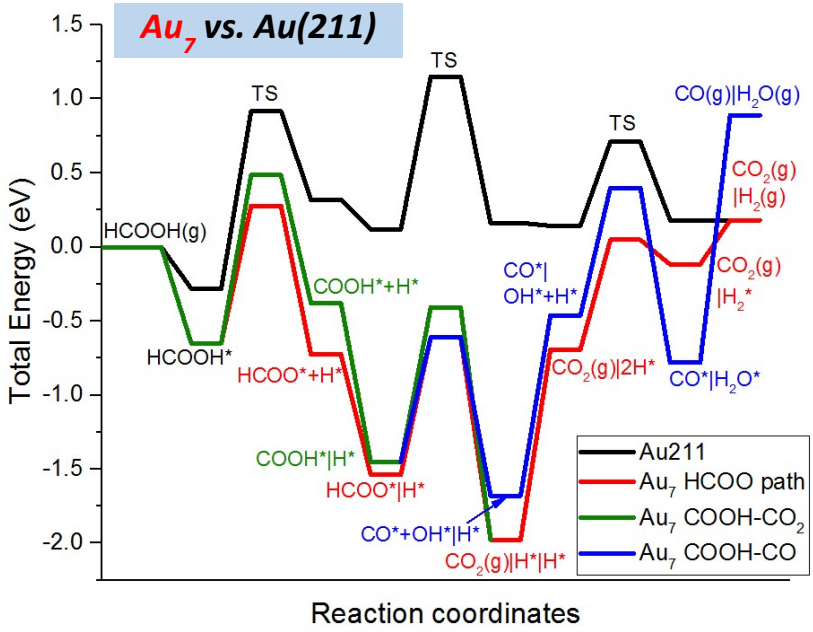

Figure S6 Potential energy diagram (PED) of HCOOH decomposition through the HCOO path (red line), COOH path leading to CO_2 formation (COOH-CO_2 path; green line) and COOH path leading to CO formation (COOH-CO path; blue line) on Au_7. PED for the HCOO path on Au(211) is shown in black, for comparison.

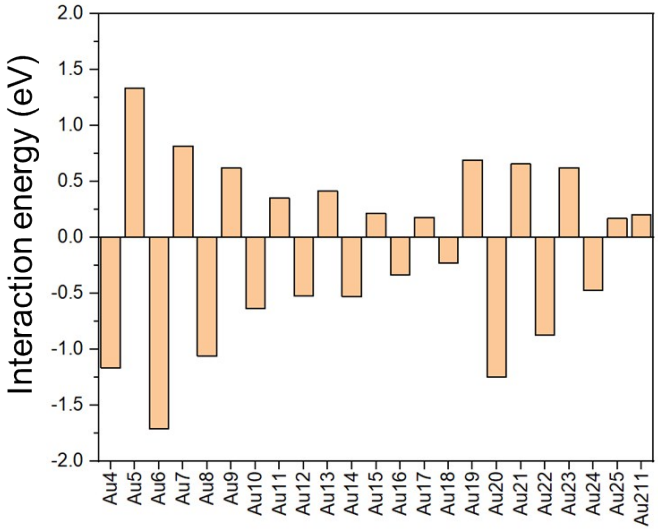

Figure S7 Interaction energy between H and HCOO on Au_n (n=4-25) clusters. Negative values indicate attractive interaction; positive values repulsive interaction.

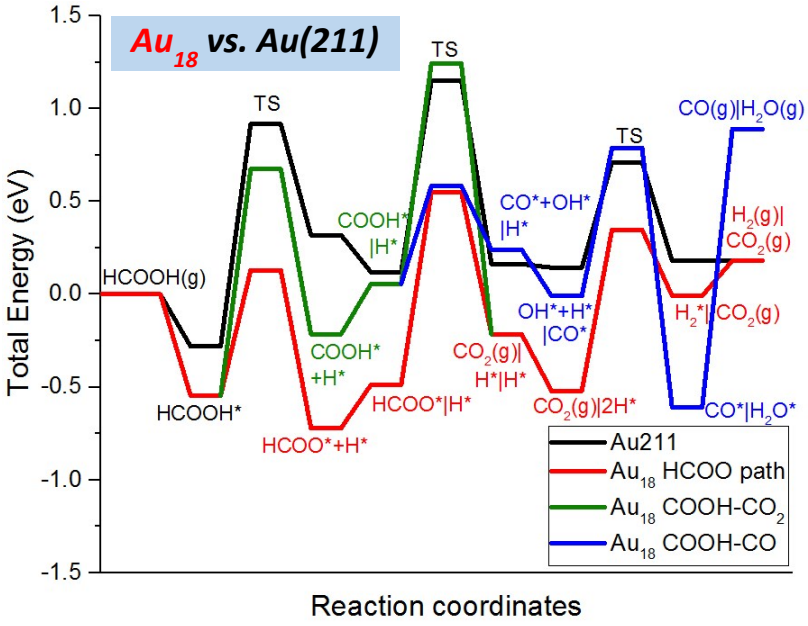

Figure S8 Potential energy diagram (PED) of HCOOH decomposition through the HCOO path (red line), COOH path leading to CO_2 formation (COOH-CO_2 path; green line) and COOH path leading to CO formation (COOH-CO path; blue line) on Au_{18}. PED for the HCOO path on Au(211) is shown in black, for comparison.

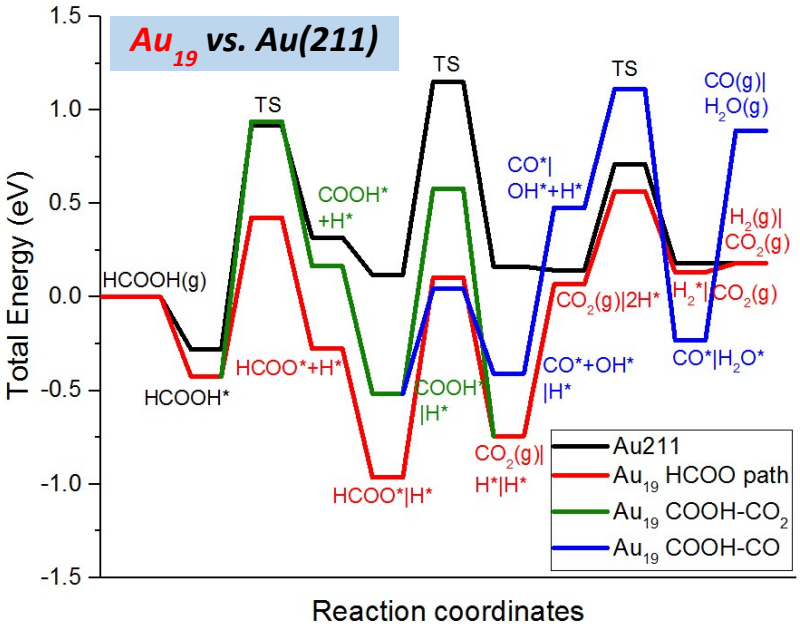

Figure S9 Potential energy diagram (PED) of HCOOH decomposition through the HCOO path (red line), COOH path leading to CO_2 formation (COOH-CO_2 path; green line) and COOH path leading to CO formation (COOH-CO path; blue line) on Au_{19}. PED for the HCOO path on Au(211) is shown in black, for comparison.

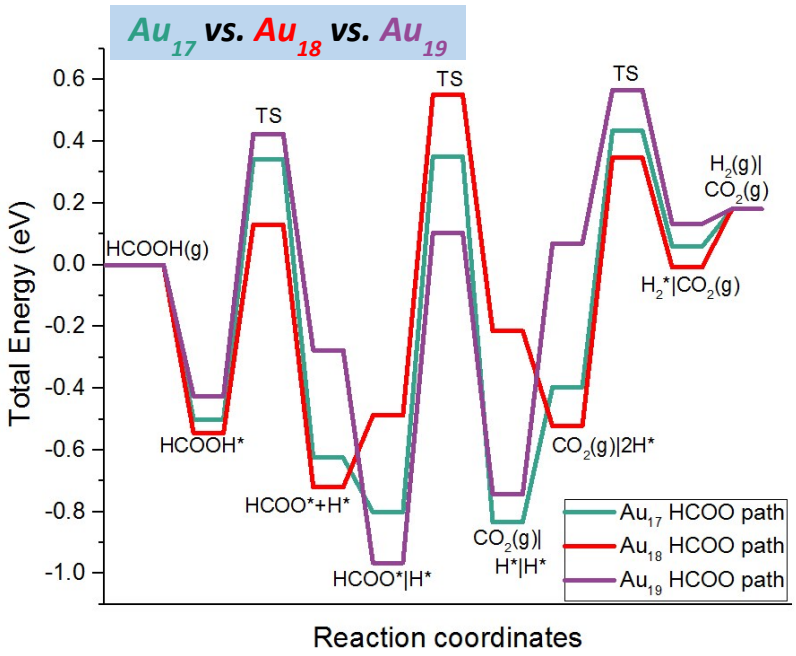

Figure S10 Potential energy diagram (PED) of HCOOH decomposition through the HCOO path on Au_{17} (green line), Au_{18} (red line) and Au_{19} (purple line).

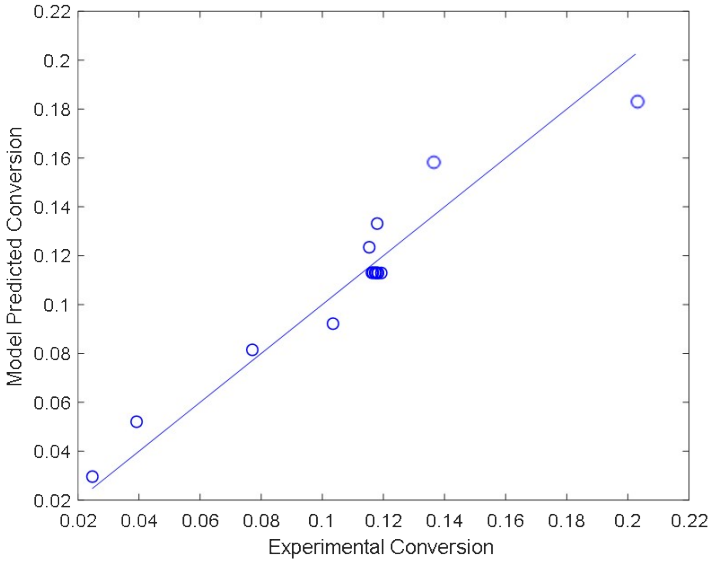

Figure S11 Parity plot between experimental conversion and model-predicted conversion obtained with adjusted parameters on Au_{18}.